Pergamon

Canadian Metallurgical Quarterly, Vol. 38, No. 5, pp. 387–396, 1999

0008-4433/00 $20.00 + 0.00

PII: S0008-4433(99)00030-0

FRACTURE OF PRECIPITATION-HARDENED COPPER ALLOY PRODUCED BY SEMI-CONTINUOUS CASTING AT ELEVATED TEMPERATURE

MICHIHARU YAMAMOTO* and TOMOJI MIZUGUCHI

Technology Development Center, Nippon Mining & Metals Co., Ltd, 1-1-2 Shirogane-Cho, Hitachi-City, Ibaraki, 317-0056 Japan

(*Received* 1 *October* 1999; *in revised form* 1 *October* 1999; *accepted* 1 *October* 1999)

Abstract—In semi-continuously cast slabs of precipitation-hardened copper alloy, internal cracks are often observed after homogenization, although those defects can not be found out after casting. It is considered that, before stress relief takes place during homogenization, thermal stresses generated in the slab during casting will exceed the fracture stress. It is of interest to understand how internal stresses of slabs will affect the fracture during homogenization. Fracture temperatures of the material under static tensile stresses are investigated in an attempt to demonstrate the fracture evolved during homogenization. © 2000 Canadian Institute of Mining and Metallurgy. Published by Elsevier Science Ltd. All rights reserved.

Résumé—Dans les brames d'alliage de cuivre durci par précipitation et coulées en semi-continu, on observe souvent des fissures internes après homogénéisation, bien qu'on ne trouve pas ces défauts après la coulée. On considère que les contraintes thermiques générées dans la brame lors de la coulée vont excéder la contrainte de rupture lors de l'homogénéisation, avant que l'effet de relaxation puisse se produire. Il est intéressant de comprendre de quelle manière les contraintes internes des brames affecteront la rupture lors de l'homogénéisation. On a étudié les températures de rupture du matériel sous contraintes statiques en traction dans une tentative de démontrer que la rupture a évolué lors de l'homogénéisation. © 2000 Canadian Institute of Mining and Metallurgy. Published by Elsevier Science Ltd. All rights reserved.

INTRODUCTION

As the result of the recent increase in more stringent demands for the high qualities and better properties of wrought products, precipitation-hardened copper alloy (Alloy 7025 i.e. Cu–2.5 wt% Ni–0.50 wt% Si–0.15 wt% Mg) with its high mechanical and electrical properties has widely been used for the electrical and electronic segments. The slabs of this alloy are generally produced by semi-continuous casting and are homogenized prior to hot rolling.

In the casting process, the stress, caused almost entirely by the volumetric expansion and contraction accompanying the change of thermal gradients within the slab, generates in the slab. It would be generally true that tensile stresses occur in the cooler regions because of the contraction restraint provided by the adjacent hotter regions and compressive stresses occur in the hotter regions. If those stresses generated during casting exceed the tensile strength of the solidified metal at elevated temperature or excess plastic strains induced due to such a non-uniform heat extraction occur during cooling, transverse surface cracks [1, 2, 3] or halfway cracks [4] will take place, depending on cooling conditions as well as mechanical properties of the metal solidified. Various investigations with respect to hot ductility accompanied with grain boundary precipitation have been carried out to understand the mechanism of crack formation during continuous casting in steels [5, 6, 7]. There are invariably sulfides, oxides, nitrides, and/or carbides at the boundaries which will act as stress concentrators and favor cavitation and crack formation in steels. The chemical composition and size distribution of such inclusions and precipitates as well as the grain size of cast alloy must, therefore, contribute to the evolution of transverse and halfway cracks. On the other hand, it is desirable to reduce the stress level in the cast slab itself by controlling cooling conditions. In terms of continuous casting process, it is considered that the control of the secondary cooling flow is most effective in reducing transverse cracking.

In the case of precipitation-hardened copper alloy such as alloy 7025, internal cracks are often observed after homogenization, although those defects can not be found out after casting. Hence, it is considered that thermal stresses generated in the slab during casting will exceed the fracture stress before stress relief takes place during homogenization.

*Author to whom correspondence should be addressed. Tel.: +81-294-23-7269; Fax: +81-294-23-7179. E-mail: michiyan@nikko-metal.co.jp.

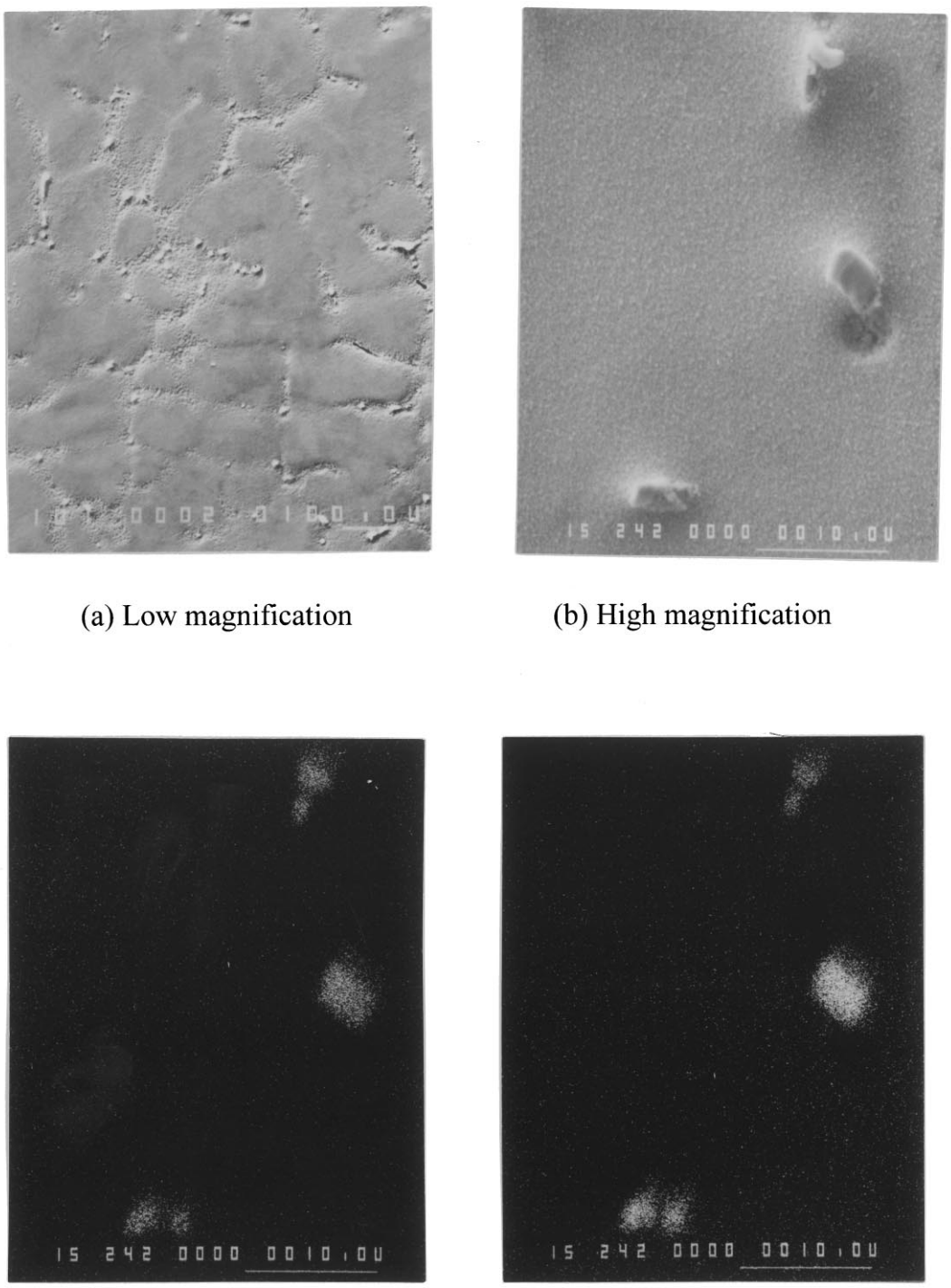

Fig. 1. Photomicrographs of as-cast specimen and results of analysis for particles precipitated during casting; Ni and Si are detected from particles precipitated. (a) and (b); SEM, (c) and (d); EPMA.

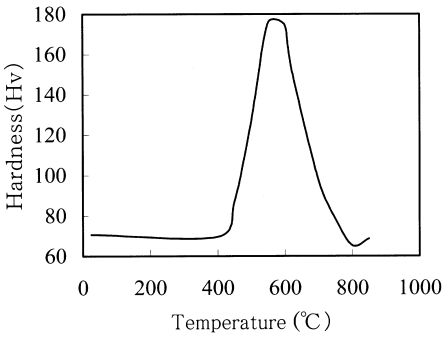

Fig. 2. Vickers hardness of specimens vs temperature.

Furthermore, those thermal stresses of casting slabs must affect the evolution and the propagation of internal cracking during hot rolling post to homogenization.

It is of interest to understand how internal stresses, generated during continuous casting, and the change of mechanical properties due to precipitation, will affect the fracture during homogenization. In an attempt to demonstrate the fracture evolved during homogenization, fracture temperatures of the material under static tensile stresses within the elastic limit, were investigated using a Gleeble thermo-mechanical simulator. The fracture mechanism of semi-continuously cast alloy 7025 during homogenization is also discussed.

Table 1. Chemical composition of alloy 7025 used in the experiment

wt% (except for S and O)					
Cu	Ni	Si	Mg	S	O
Rem.	2.48	0.54	0.08	4 ppm	< 1 ppm

Table 2. Heating conditions of specimens in the static tensile stress test*

	Heating rates	
Condition	RT-420°C	420–880°C
Homogenizing	7°C/min	4°C/min
2 times	14	8
3 times	28	16
10 times	70	40
100 times	700	400

* RT: room temperature.

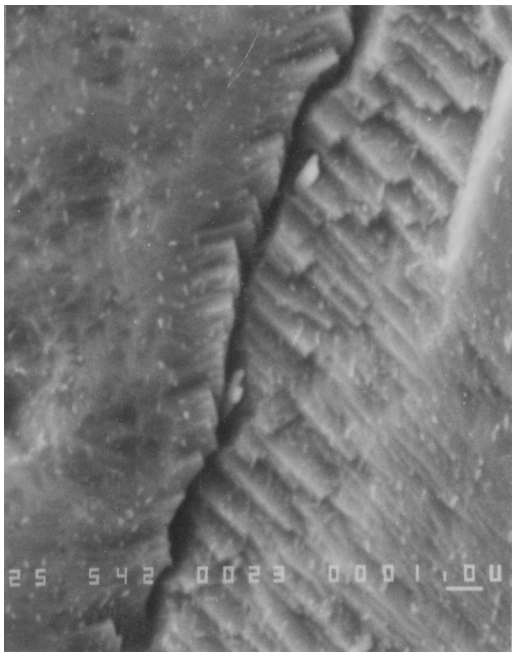

Fig. 4. Microstructure of specimen heated to 750°C at the same rate of homogenizing.

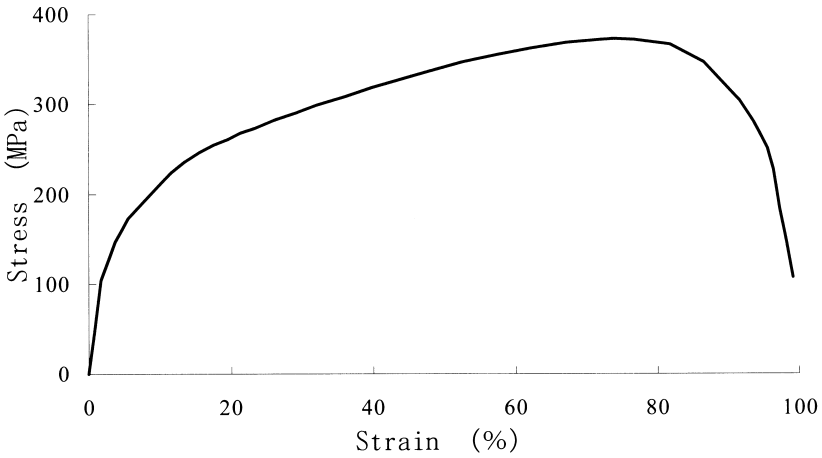

Fig. 3. Stress–strain curve of as-cast specimen at the strain rate of 0.25/s.

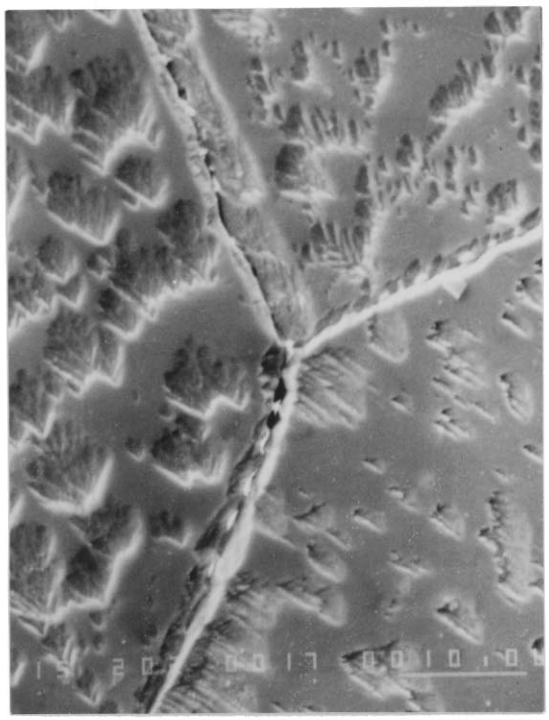

(a') High magnification in (a)

Fracture surface

(a) Fracture at 632 ℃
Static tensile stress 65 MPa

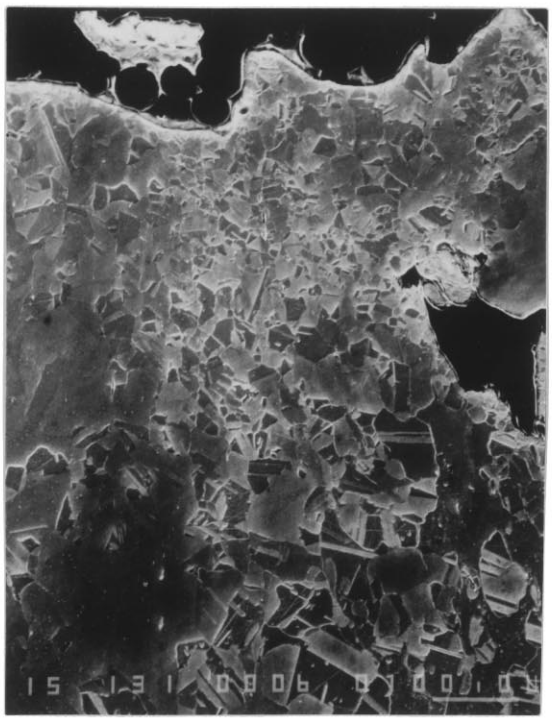

(b) Fracture at 812℃
Static tensile stress 49 MPa

Fig. 5. Scanning electron micrographs of cross section perpendicular to fracture surfaces in the static tensile test; Failed at (a) 632°C and (b) 812°C.

EXPERIMENTAL PROCEDURE

Sample preparation

In the semi-continuous casting process of copper alloy, molten metal prepared in the induction furnace is poured into the mold through a tundish, which has a submerged graphite nozzle in its bottom with the stopper needle controlled by hand-operated screw, and the heat of the metal is mainly extracted from the mold wall at first. The metal, partially solidified from its surface in the mold of copper plated with chromium, is vertically withdrawn from the bottom of the oscillating mold at the rate of 100 mm/min. Sprays of the secondary cooling water, installed just below the mold, impinge on the descending slab and the metal is perfectly solidified below the bottom of the mold within the secondary cooling zone. The casting is terminated when the length of slab becomes more than a few meters. Test pieces are cut from a semi-continuously cast slab, 200 mm in thickness, 500 mm in width, and 3500 mm in length.

The chemical composition of an alloy 7025 used for the investigation is shown in Table 1. From slices of the cast slab, test pieces for a Gleeble test, 10 mm in diameter and 100 mm in length, were machined along with the direction perpendicular to the wide surface of the cast slab. The cross-sectional area of the as-cast specimen was etched by ferric chloride and analyzed by EPMA. Micrographs of the as-cast specimen are shown in Fig. 1. Particles of (NiSi) are observed between dendrite arms due to the evolution during solidification.

To understand the change of mechanical properties during homogenization, as-cast specimens were heated to some elevated temperature at the same rate as the homogenizing condition, cooled down to the ambient temperature by air quenching and then hardness tests of those heat-treated specimens were carried out. Results shown in Fig. 2 indicate that specimens, heated between 400 and 750°C, are hardened. Micrograph of specimen heated to 750°C is presented in Fig. 3 and exhibits very fine particles of (NiSi). The rise of hardness for specimen heated between 400 and 750°C is due to precipitation of such fine particles.

Experimental design

In order to control temperatures of the test piece in a Gleeble test, the thermocouple is attached to the center portion of specimens. The tension-tests in the vacuum atmosphere were carried out in the Model 1500 Gleeble, which can subject specimens to various types of thermal cycles.

Tensile tests of as-cast specimens were conducted first to measure the mechanical properties. In the second step, effects of heating rates for hot ductility during homogenization were investigated. Specimens under static tensile stresses were heated at the various rates and the temperatures, at which specimens failed, were measured. This experiment is called the static tensile stress test. Tensile tests at elevated temperature were finally conducted in order to compare the results with those of the static tensile stress tests. This experiment is called the hot tensile test.

In order to decide applied stress level for specimens in the static tensile stress test, a tensile test of as-cast specimen was conducted at room temperature and the stress-strain curve is shown in Fig. 4. The ultimate tensile strength and the elastic limit of as-cast specimens are 350 and 100 MPa, respectively. Static tensile stresses within 100 MPa were, therefore, applied in the static tensile stress test.

To simulate the internal stress generated during casting, specimens applied with some amount of static tensile stresses were heated from room temperature to 880°C in accordance with the ordinary homogenizing condition, which is at the rate of 7°C/min to 420 and 4°C/min from 420 to 880°C. This heating curve simulated homogenizing condition is called homogenizing. In those tests, temperatures and stresses for specimens are recorded and it is confirmed that the static tensile stress applied is controlled within $\pm$ 3%. Since specimens under static tensile stresses failed at some elevated temperature, those static tensile stresses, as a function of fracture temperatures, are obtained in the simulated tests of fracture during homogenization. Photographs of the initial (S_i) cross-sectional area and the fracture surface (S_f) were taken in order to measure the reduction of area (RA) at fracture ($=(S_i-S_f)/S_i \times 100(\%)$) which can provide

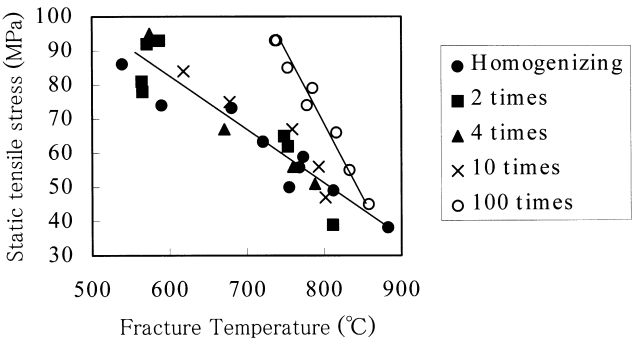

Fig. 6. Relationship between fracture temperature and static tensile stress for specimens, heated at the various rates under static tensile stresses.

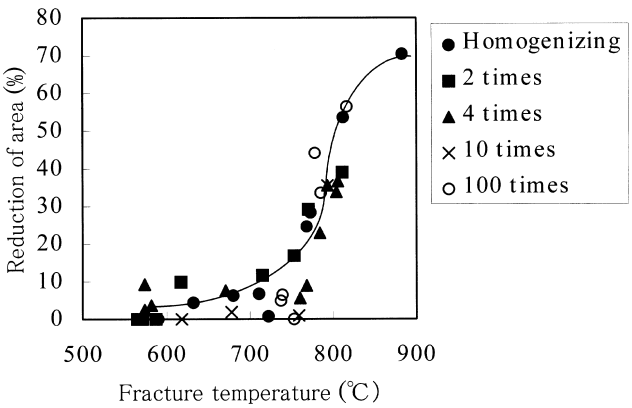

Fig. 7. Relationship between fracture temperature and reduction of area for as-cast specimen, heated at the various rates under static tensile stresses.

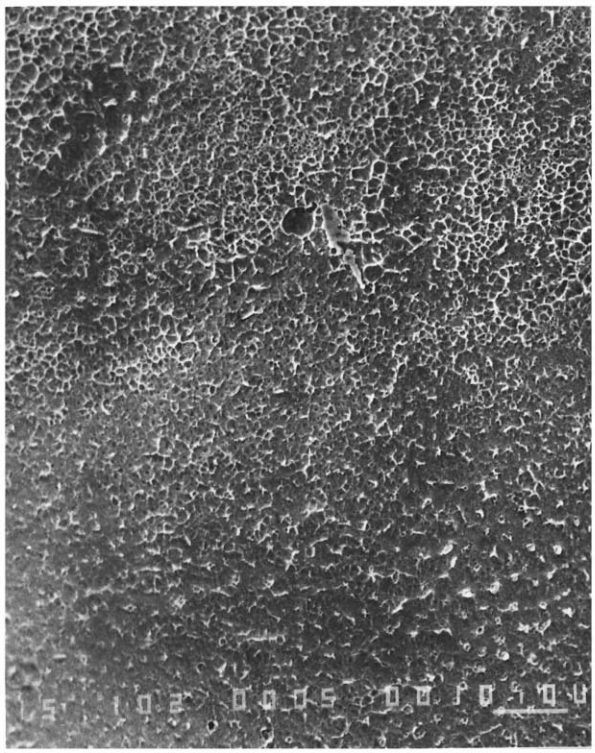

(a) Fracture at 590 ℃
Static tensile stress 76 MPa

(b) Fracture at 632 ℃
Static tensile stress 65 MPa

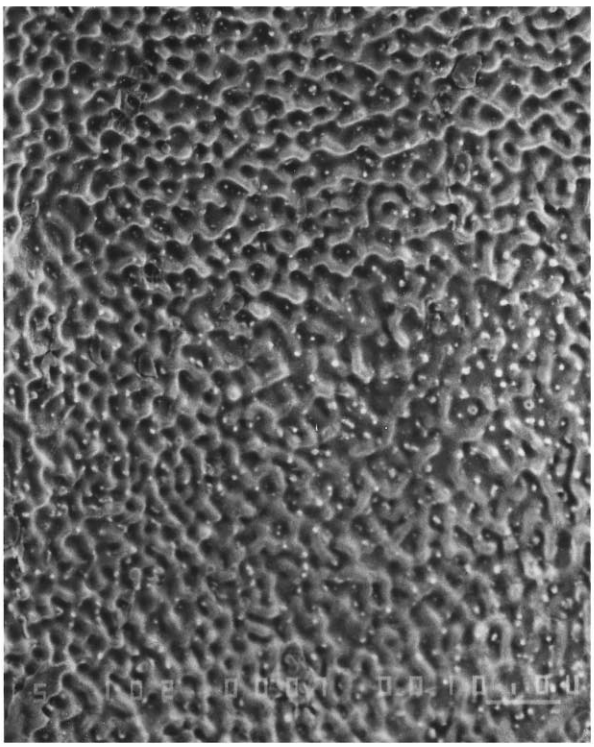

(c) Fracture at 755 ℃
Static tensile stress 50 MPa

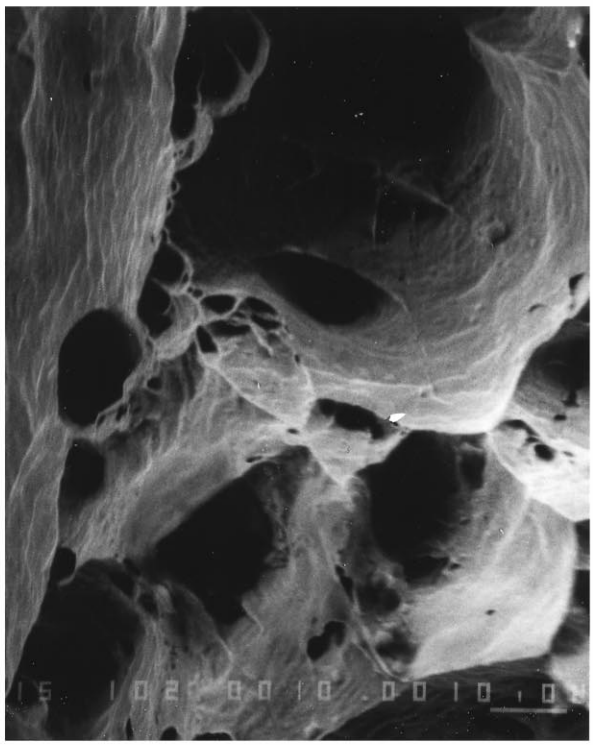

(d) Fracture at 814 ℃
Static tensile stress 39 MPa

Fig. 8. Comparison of fracture surfaces of specimens failed under the various static tensile stresses at elevated temperature: heating rate 7°C/min (RT-420°C), 4°C/min (420°C—fracture temperature); fracture at (a) 590°C, (b) 632°C, (c) 755°C, (d) 814°C.

quantitative information for hot ductility. Furthermore, photomicrographs of fracture surfaces were observed, using scanning electron microscopy (SEM).

RESULTS AND DISCUSSION

Comparison of micrographs for static tensile tests

As-cast specimens, under various static tensile stresses heated at the simulated homogenizing condition, failed at stress-dependent different temperatures during heating. The cross-sectional areas perpendicular to the fracture surface were observed by SEM. Micrographs of specimens failed at the regions of low and high ductility, are presented in Fig. 5. For the specimen failed at 632°C (low ductility region), it is likely that intergranular failure takes place and microvoid at the grain boundary can also be observed. It is noted in steel that intergranular failure in the region of low ductility is caused either by grain boundary sliding and cavitation at the grain boundary, or by the formation of a thin film of deformation induced ferrite at the austenite grain boundary [6]. In this precipitation hardened copper alloy, such intergranular failure at the intermediate temperature might be governed by grain boundary sliding due to wedge crack and cavitation.

On the other hand, micrograph of specimen failed at 812°C (high ductility region) exhibits fine structure along with fracture surface probably due to dynamic recrystallization. It is noted that one way to achieve a high driving force from grain boundary migration will be dynamic recrystallisation.

Therefore, the dependence of hot ductility on temperature and applied tensile stress will be determined by the competition between recrystallisation and precipitation at the grain boundary. If dynamic recrystallisation can dominate, the stress concentration at the grain boundary is relaxed and the ductility will become high, because the existing precipitation and any voids are left inside the new grains. In the brittle fracture region, it is generally believed that vacancies will diffuse to precipitate particles on the grain boundaries, and cavities and microvoids are nucleated at geometrical irregularities or grain boundaries where high stress concentration could develop.

Effects of heating rates during homogenization for hot ductility

As-cast specimens applied with some amount of static tensile stresses were heated from room temperature to 880°C at various heating rates, ranged from the same rate of the previous experiment, i.e. the simulated homogenizing condition, to 100 times faster. Heating conditions of specimens in the static tensile stress test are listed in Table 2. The temperature at which the specimen under static tensile stress failed is defined as fracture temperature. Fracture temperatures as a function of static tensile stresses were obtained for various heating rates. The reduction of area at fracture and fracture surfaces were also measured.

Relationship between static tensile stresses and fracture temperature for the various heating rates is shown in Fig. 6. If the heating rates are ranged within 10 times faster than the ordinary homogenizing condition, it is likely that fracture temperatures of specimens under static tensile stresses are almost independent of those heating rates. However, fracture temperatures of specimens under the same static tensile stresses heated at the rate of 100 times faster do tremendously rise in the relatively low temperature and finally become close to values of other specimens heated at the slower rates. Specimens heated at the rates of 10 times faster, whose rate from 400 to 700°C correspond to 0.7°C/s, can still have enough time to give a rise to precipitates on the grain boundaries and to migrate cavitation around precipitates. Once precipitates are formed on the grain boundaries, applied stresses concentrate around those precipitates in accordance with the rising temperature. Consequently, the brittle intergranular fracture due to grain boundary sliding will take place when the applied stress level is beyond the elastic limit.

Reductions of area as a function of fracture temperatures for specimens failed in the static tensile stress

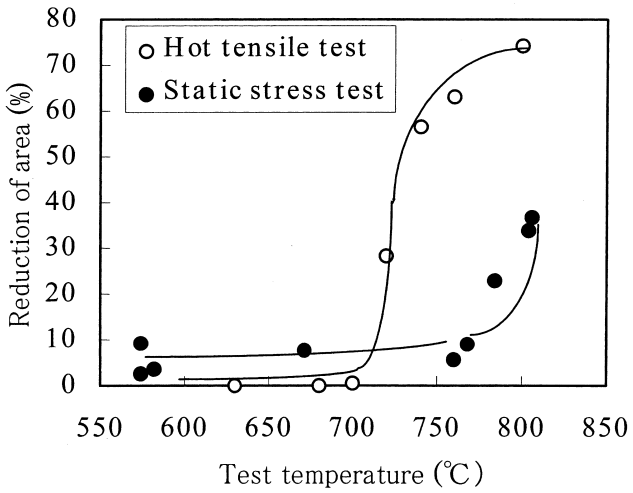

Fig. 9. Comparison of reduction of area at fracture between hot tensile-test at the strain rate of 0.25/s and static stress test.

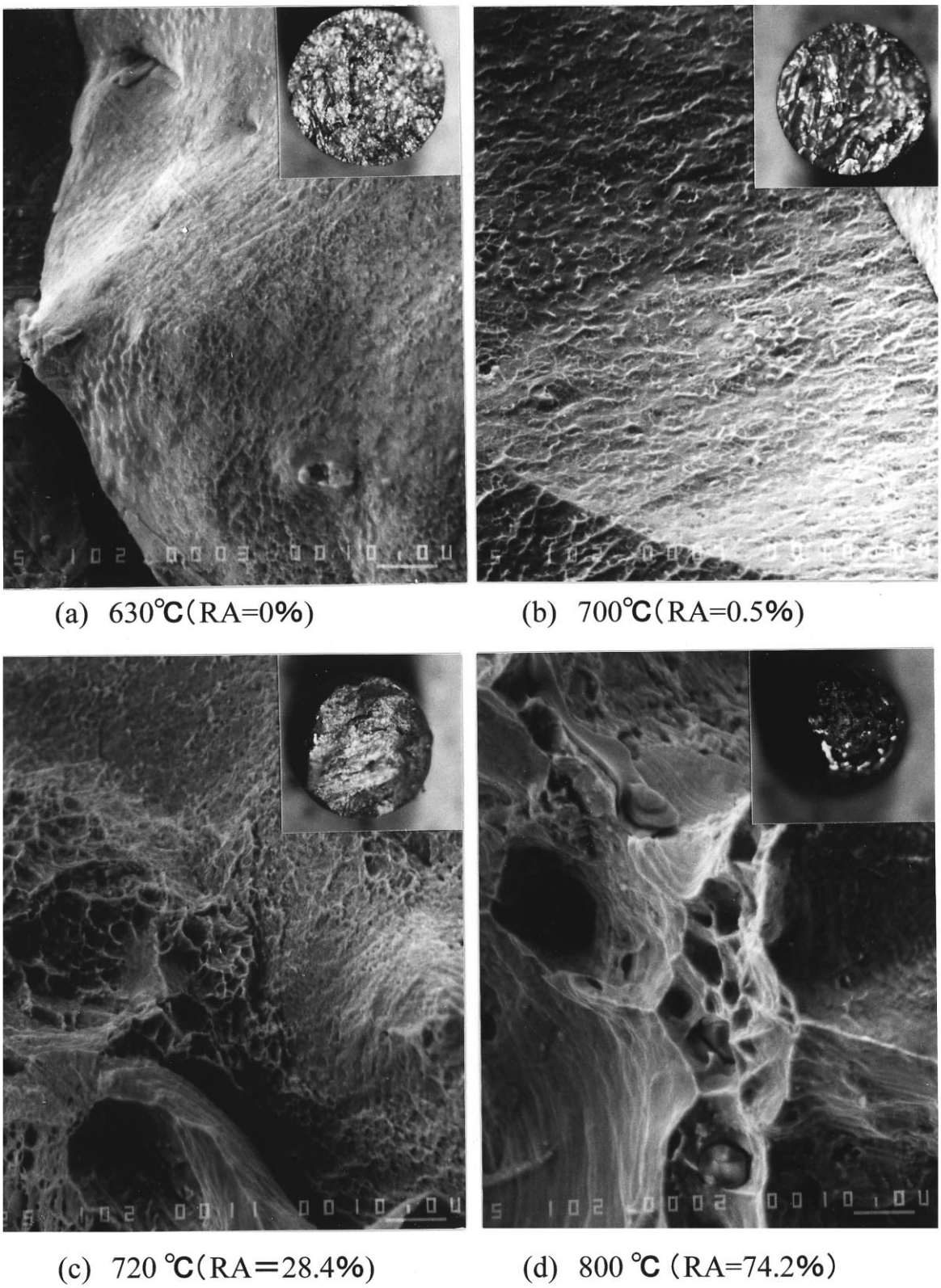

Fig. 10. Comparison of fracture surfaces hot tensile-test specimens at the various temperatures: (a) 630°C (reduction of area (RA) = 0%); (b) 700°C (RA = 0.5%); (c) 720°C (RA = 28.4%); and (d) 800°C (RA = 74.2%).

test exhibit in Fig. 7 and photomicrographs of the fracture surface are presented in Fig. 8. At the low fracture temperature of less than 760°C, values of reduction of area are less than 20%, being independent of heating rates and the corresponding microstructures indicate the faceted and dimple structure with small precipitate particles. It is also observed that at such a low temperature the cavity spacing λ increases with increasing fracture temperature or decreasing applied tensile stresses. The tips of each uneven surface in Fig. 8(c) are relatively smooth probably due to the action of surface diffusion in the fracture surface [8]. While the fracture surface at the high temperature i.e. 814°C in Fig. 8(d) exhibits rupture pattern with large holes and undulation, reductions of area for the fracture temperature of more than 760°C gradually increase with rising temperatures.

Comparison between the static tensile stress test and the hot tensile test

To compare results of the static tensile stress test with those for dynamic tensile stresses (the hot tensile test), tensile tests at elevated temperature were also conducted. As-cast specimens were heated at the rate of 4 times faster than the ordinary homogenizing condition to the experimental temperature at which hot-tensile tests were carried out at the strain rate of 0.25/s. The ultimate tensile strengths at elevated temperature were obtained and reductions of area at fracture and photomicrographs of fracture surfaces were measured.

Results of the static tensile stress test were compared with those of the hot tensile test to evaluate difference between the deformation processes. Reduction of area for the hot tensile test, accompanied with those of the static tensile stress test, are shown in Fig. 9. The transition temperature between brittle transgranular fracture and ductile fracture is defined as the point at which reduction of area is 20%. In the hot tensile test the transition temperature is at 720°C, while for the static tensile stress test it is at 760°C.

The fracture-mechanism maps for various metals presented by Ashby *et al*. [9] show the fields of dominance of a given micromechanism of fracture with tensile stress and temperature. Most maps of fcc metals exhibit four principal fields, corresponding to ductile fracture, transgranular creep fracture, intergranular creep fracture and rupture. It is noted that the boundary of homologous temperature ($=T/T_m$, T_m = melting temperature), between rupture due to dynamic recrystallisation and intergranular creep fracture for OFHC copper, decreases with increasing normalized tensile stress defined as the nominal stress in a creep or tensile test over Young's modulus. Since the ultimate tensile stress at the transition temperature in the hot tensile test is 120 MPa and 2 times higher than the static tensile stress of specimen at the same fracture temperature in the static tensile stress test, it can be assumed that such high tensile stress in the hot tensile test helps to prevent localized deformation even if cavities diffuse in to the grain boundaries during heating.

Fracture surfaces of the hot tensile test for the various test temperatures are also presented in Fig. 10. At test temperature lower than 700°C, fracture surfaces are smooth faceted and show dimple pattern, while those at test temperature higher than 720°C show rupture and undulations that appear to increase with rising test temperatures.

SUMMARY

In order to simulate the fracture taking place during homogenization, static tensile stress and hot tensile tests of semi-continuously cast slabs of precipitation-hardened copper alloy 7025 were conducted using a Gleeble thermo-mechanical simulator. The results obtained are summarized as follows.

1. In the static tensile stress test simulating cracking during homogenization, fracture temperatures rise with decreasing static tensile stresses. Fracture patterns at elevated temperature are classified into brittle intergranular for low temperature and rupture due to dynamic recrystallisation at high temperature.
2. If the heating rates are relatively slow, ranged within the heating rate of 10 times faster than the ordinary homogenizing condition, fracture temperatures are almost independent of heating rates. Fracture temperatures of specimens heated at the rate of 100 times faster are relatively higher in the brittle intergranular region even at the same static tensile stresses and tend to be close to those values in the rupture region of specimens heated at the lower rates.
3. To evaluate the differences between the deformation processes, results of the static tensile stress test were compared with those of hot tensile tests. In the hot tensile test, the transition temperature between brittle transgranular fracture and ductile fracture due to dynamic recrystallisation is at 720°C. This is relatively low when compared to the value of specimen failed in the static tensile stress test. It can be assumed that high tensile stress in the hot tensile test helps to prevent localized deformation even if vacancy diffusion to the grain boundaries takes place during heating.

Acknowledgements—Helpful comments, suggestion, discussion and encouragement were given by Professor Alexander McLean, University of Toronto, Masanori Iwase, Kyoto University and Dr Tsuguo Ogura, Nikko Techno Service Co. Ltd. The authors wish to thank Messrs. Osamu Kato and Masanori Kato, Technology Development Center, Nippon Mining & Metals Co. Ltd., for their aid in progress of experiments.

REFERENCES

1. Turkdogan, E. T., I & SM, May 1989, Vol. 16, p. 61.

2. Suzuki, H. G., Nishimura, S., Imamura, J. and Nakamura, Y., *Tetu-to-Hagane*, 1981, **67**(8), 1180.
3. Coleman, T. H. and Wilcox, J. R., *Mater. Sci. & Tech.*, 1985, **1**, 80.
4. Brimacombe, J. K., *Can. Metall. Quart*, 1976, **15**(2), 163.
5. Cardoso, G. I. S. L. and Yue, S., Proceedings of Mech. Working & Steel Proc., 1989, p. 585.
6. Mintz, B., Yue, S. and Jonas, J. J., *Inter. Mat. Rev.*, 1991, **36**(5), 187.
7. Lankford Jr, W. T., *Metall. Trans.*, 1972, **3**, 1331.
8. Goods, S. H. and Nix, W. X., *Acta Metall.*, 1978, **26**, 739.
9. Ashby, M. F., Gandhi, C. and Taplin, D. M. R., *Acta. Metall.*, 1979, **27**, 699.